Biomedical Signal Processing and Control 34 (2017) 64–73

Contents lists available at ScienceDirect

Biomedical Signal Processing and Control

journal homepage: www.elsevier.com/locate/bspc

Motor unit profile: A new way to describe the scanning-EMG potential

Íñigo Corera*, Armando Malanda, Javier Rodriguez-Falces, Sonia Porta, Javier Navallas

Department of Electrical and Electronic Engineering, Public University of Navarra, Pamplona, Spain

ARTICLE INFO

Article history:
Received 8 August 2016
Received in revised form
21 November 2016
Accepted 20 December 2016
Available online 16 February 2017

Keywords:
Electromyography (EMG)
Scanning-EMG
Quantitative EMG
Turns

ABSTRACT

The motor unit profile, a representation of the trajectories of positive and negative turns of a scanning-EMG signal, is a new way to characterize the motor unit potential. Such characterization allows quantification of the scanning-EMG signal's complexity, which is closely related to the anatomy and physiology of the motor unit. To extract the motor unit profile, an algorithm that detects the turns of the scanning-EMG signal and links them using point-tracking techniques has been developed. The performance of this algorithm is sensitive to three parameters: the turn detection threshold, the maximum tracking interval threshold, and the trajectory purge threshold. Real scanning-EMG signals have been used to analyze the algorithm's behavior and the influence of the algorithm's parameters and to determine which parameter values provide the best performance.

1. Introduction

Quantitative analysis of the motor unit potential (MUP) waveform consists in defining waveform features that allow characterization of several aspects of MUPs, such as, their size, length and complexity. Several MUP parameters described in the literature [1–3] are duration, amplitude, area, size-index, rise-time, phases, turns, and irregularity coefficient. MUP quantification has important applications in clinical neurophysiology, where it can be used to obtain estimates of the normal values for the parameters, and in diagnostic techniques based on detecting deviation of recorded MUP parameters from normal values [2]. In this way MUP quantification analysis makes it possible to relate changes in MUP waveform with changes in the physiological and anatomical properties of the motor unit (MU), knowledge that is useful to detect neuro-muscular pathologies.

A step forward in MUP quantification analysis has been enabled by the electrophysiological technique of scanning-EMG, which consists in recording the MUP from multiple points along a linear corridor [4]. Scanning-EMG employs two needle electrodes: the trigger electrode, which is placed to record the activity of a particular motor unit; and the scanning electrode, which is attached to a stepper motor that pulls the needle along the linear corridor in small increments. In each recording site, when the trigger electrode detects the firing of the MU, the scanning electrode records a MUP. In this way, the scanning electrode provides synchronized recordings of all the MUPs from a single MU. The scanning-EMG recording results in a bidimensional MUP that varies both in time and in space, as depicted in Fig. 1(a) and (c).

When applied to normal muscles, scanning-EMG allows determination of structural MU properties that are not accessible with other electrophysiological techniques. Examples of such structural properties are MU fractions and silent areas [5–7], which are essential to investigate the architecture of the MU territory. Structural complexity has been addressed by defining several parameters in scanning-EMG recordings [6,7]: length of the MU territory, number of MU fractions, temporal delay between fractions, number of polyphasic fractions, etc. However, because these parameters do not make effective provision for the bidimensional information of the scanning-EMG signal, they are insufficient to fully characterize complexity throughout the whole MU territory.

In the present study, to resolve the above limitation, a new characterization of the scanning-EMG signal, the MU profile, is proposed. The MU profile is conceived to provide the trajectories of the crests and valleys of the bidimensional MUP (Fig. 2). In essence, the algorithm applies point tracking techniques [8,9] imported from image processing theory to link the turns extracted from individual MUPs in such a way that smooth trajectories are formed. In the following sections, the algorithm to extract the MU profile is detailed, and experiments based on real scanning-EMG signals are analyzed. The effects of the algorithm's parameters and the usefulness of the MU profile are discussed.

* Corresponding author.
E-mail address: inigo.corera@unavarra.es (Í. Corera).

http://dx.doi.org/10.1016/j.bspc.2016.12.020

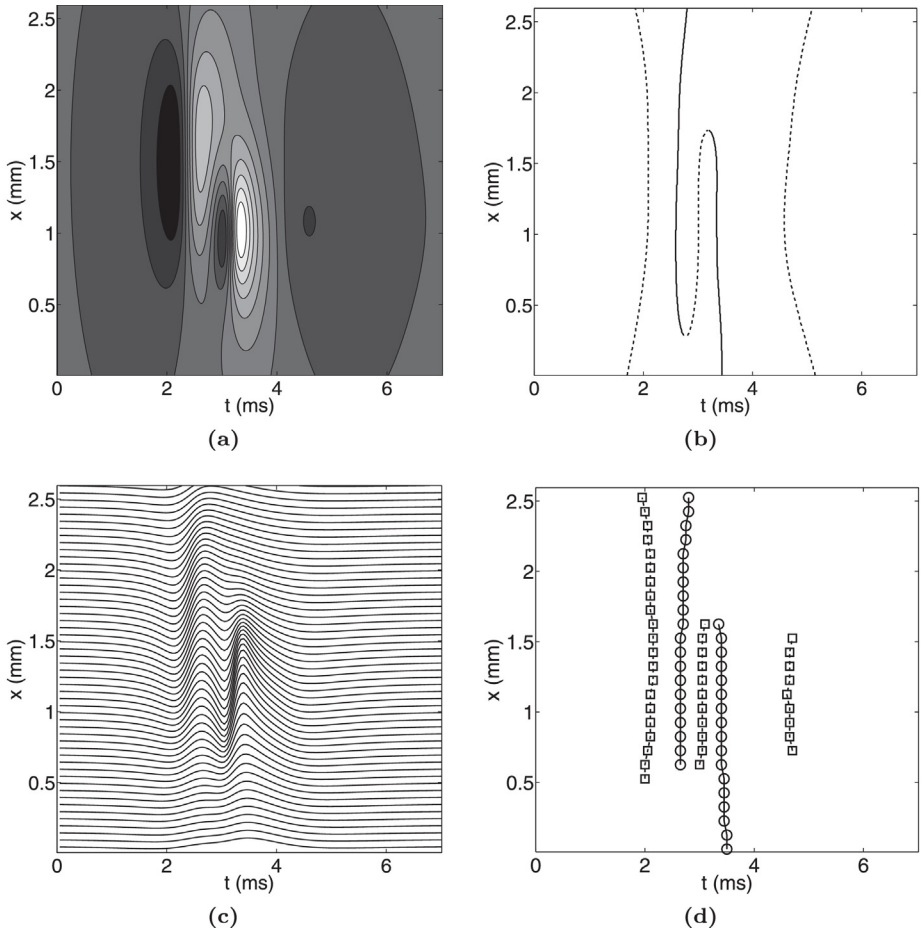

Fig. 1. Representation of a simulated scanning-EMG signal and its MU profile: (a) bi-dimensional continuous bioelectric potential $V(x, t)$ varying in time and space, with peaks and depressions related to depolarized and repolarized regions of the MUP. Note that the spatial dimension is the depth of the scanning electrode; (b) crests and valleys of the continuous bioelectric potential corresponding to the local maxima (solid lines) and the local minima (dotted lines), i.e., to the set of points satisfying (1); (c) the scanning-EMG signal as a discrete version of the bi-dimensional continuous bioelectric potential, essentially a MUP observed at different locations along a linear corridor; (d) positive turns (circles) and negative turns (squares) corresponding to local maxima and minima, respectively, extracted at each spatial recording position of the scanning-EMG signal. Observe the direct visual correspondence with the crests and valleys in (b).

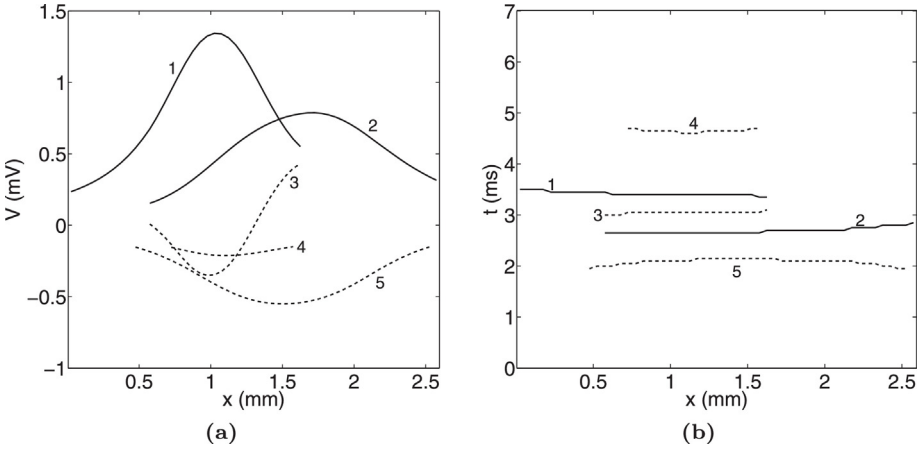

Fig. 2. Representation of the MU profile of the scanning-EMG signal presented in Fig. 1: (a) projection of the trajectories in the amplitude-space plane gives a view of the MUP amplitude changes across the scanning corridor; (b) projection of the trajectories in the time-space plane gives a view of the MUP delay and synchronization among MU fractions. Trajectories are numbered from 1 to 5 to show their correspondence in both projections. Note that the trajectories composed of positive turns (solid lines) are associated with the crests, and trajectories composed of negative turns (dotted lines) are associated with the valleys of the scanning-EMG signal.

2. Materials and methods

2.1. MU profile mathematical basis

In a scanning-EMG signal, the MUP is a bi-dimensional continuous bioelectric potential $V(x, t)$, where x is the position of the recording needle along the corridor and t is the time variable (Fig. 1(a)). The MU profile is defined as the mathematical locus of the points within the MUP duration limits satisfying:

$$\frac{\partial V(x,t)}{\partial t} = 0 \tag{1}$$

Thus, the MU profile is the set of the crests and valleys of the MUP, where crests and valleys are the set of smooth sequences in the spatial dimension of local maxima and minima of $V(x, t)$ extracted in the temporal dimension (Fig. 1(b)).

In practice, a scanning-EMG signal is the recording of a MUP in discrete spatial locations along a linear corridor. These locations are equally spaced, usually 50 μm apart, from each other [10]. The set of MUPs recorded along the corridor can be regarded as a spatially and temporally sampled version of $V(x, t)$ (Fig. 1(c)). Hence, the scanning-EMG recording can be expressed as $V[k, n]$, $1 \le k \le K$, $1 \le n \le N$, where K is the number of recording sites along the scanning corridor, and N is the number of time samples of the recording. When dealing with the discrete-time version of the MUP, the points that satisfy (1) are the turns of the MUP extracted for each spatial position, where local maxima correspond to positive turns and local minima correspond to negative turns. Hence, the discrete-space-time version definition for the MU profile is the set of trajectories formed by linking through the spatial dimension the turns extracted from each spatial recording position (Figs. 1(d) and 2).

In each of the recording locations the set of turns of the MUP can be extracted:

$$T = \{t_k^q\} = \{(k, n_k^q, V[k, n_k^q])\}; \quad 1 \le k \le K; \quad 1 \le q \le Q_k \tag{2}$$

where t_k^q is the qth turn detected in the kth recording site, which is represented by three coordinates, corresponding to the position k, the time of occurrence of the turn n_k^q, and the amplitude of the turn $V[k, n_k^q]$. Q_k is the number of turns in the MUP from the kth recording site. Note that at each recording location the MUP may have a different number of turns, since the complexity of the MUP may vary across the recording corridor [11,10] (Fig. 3).

To link the turns into trajectories, point tracking techniques can be used [12]. Hence obtaining the MU profile is equivalent to performing a point tracking over the set of detected turns. The set of trajectories, which is the MU profile, is (Fig. 2):

$$P = \{p_k^i\} = \{(k, m_k^i, V[k, m_k^i])\}; \quad k_1^i \le k \le k_2^i; \quad 1 \le i \le I \tag{3}$$

where p_k^i is the turn at position k of the ith trajectory, which is represented by three coordinates: the position k, the time of occurrence of the turn m_k^i, and the amplitude of the turn $V[k, m_k^i]$; k_1^i and k_2^i are the initial and final positions of the ith trajectory, and I is the number of trajectories found.

Point tracking techniques make it possible to solve the correspondence problem, that is, to identify the same characteristic point in different 2D-frames of a video sequence [8]. Each frame of the video sequence corresponds to a certain time instant where a set of characteristic points are detected. Each of these points is characterized by two coordinates representing its position in the 2D-frame. The challenge is to find the trajectories of the points as they change position from one frame to the next.

One of the main difficulties of point tracking are occlusions. In a dynamic video scene, characteristic points can appear and disappear in certain frames [9]. Thus, in order to obtain adequate point tracking when occlusions can occur, the point tracking algorithm must allow trajectories to begin or end in any frame. The greedy exchange algorithm [8,9] satisfies this requirement and was chosen as the base for the MU profile extraction technique presented here.

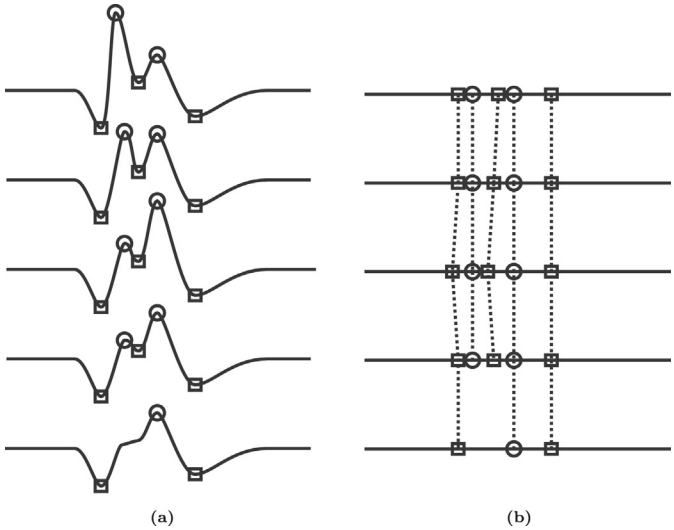

Fig. 3. (a) Five MUPs recorded in successive locations (recording sites), with their positive (circles) and negative (squares) turns identified. The amplitude of a turn can vary drastically from one recording position to the next one, however this is not the case for the time of occurrence. Note that two of the turns disappear in the last recording site; (b) the turns of each frame are represented keeping only their temporal information (excluding their amplitude) and are tracked among the five recording sites. Note the sudden disappearance of two trajectories in the last recording site.

The greedy exchange algorithm finds a set of smooth trajectories composed of the points in consecutives frames. The algorithm starts from an initial set of trajectories formed by joining the closest points (so called nearest neighbors) in consecutives frames. These initial trajectories are refined using an iterative process in which points in different pairs of trajectories are swapped and the new local smoothness of the trajectories is evaluated; the point-exchange that provides the greatest increase of the local smoothness is implemented in each iteration. This procedure ensures the maximization of the overall smoothness of the trajectories.

To solve the occlusion problem, the greedy exchange algorithm is able to work with incomplete trajectories that can finish or begin in arbitrary positions. The algorithm achieves this by using the concept of phantom points that represent absences of points in the trajectories. Thus, to obtain a set of optimal trajectories that take into account the possibility of occlusion, the algorithm exchanges both real points and phantom points between the different pairs of trajectories.

2.2. Algorithm development

MU profile extraction is divided into two main steps. The first step detects the MUP turns at each recording site of the scanning-EMG signal. Turns are the local maxima and minima of each MUP; however, in practice, only those local maxima and minima that exceed a certain threshold T_{thr} are considered valid turns [1]. This prevents the algorithm from regarding noise in the recorded signal as turns [1]. The second step uses a point tracking algorithm to join the detected turns into trajectories. The point tracking is applied separately to the set of positive turns and the set of negative turns. This precludes the possibility of linking positive and negative turns together, which would result in incorrect trajectories.

The application of point tracking techniques to the linking of turns implies that the correspondence problem must be reformulated. Each of the MUPs recorded in a particular site along the scanning corridor can be regarded as a frame, and the set of turns found for this MUP are regarded as a set of points to be linked, between frames, by the algorithm (Fig. 3(a) and (b)). Therefore, the role of the time dimension in the original formulation now corresponds to the depth of the needle in the scanning corridor (Fig. 1(c)). Another important difference is that the point tracking algorithm should work with unidimensional points, the time of occurrence of the turns, rather than bidimensional points; turns have two dimensions (besides the spatial position): the time of occurrence of the turn and its amplitude. However, the point tracking algorithm ignores the amplitude information. The rationale is that the time shift of the turns between consecutive recording sites is expected to be small, while its amplitude may vary drastically, for example, because the recording needle is much closer to or more distant from the group of fibers [13,14]. Consequently, it is easier for the algorithm to track points separated only by small time variations than to track point separated by combined time-amplitude variations (Fig. 3(a) and (b)).

In scanning-EMG, a MUP's waveform complexity can differ significantly in the different positions of the scanning corridor [11,10]. Hence, the number of detected turns may vary depending on the position (Fig. 3(c) and (d)). The use of the greedy exchange algorithm [9] ensures the ability to obtain trajectories that can begin and finish at any scanning position.

Some changes to the standard version of the greedy exchange algorithm have been implemented. The criterion used to initialize the trajectories is modified, such that turns are linked in order of occurrence in time, that is, the qth turn of each position is linked with the qth turn of the next position (Fig. 4(a)). This procedure replaces the nearest neighbor criterion used in the original algorithm to ensure that there is no temporal crossing between trajectories in the initial set of trajectories. Note that, in the reformulated conception, formation of temporarily crossed trajectories in the time-space plane is not allowed. This is because sequential turns detected from a MUP must have alternating signs; a local minimum is always followed by a local maximum, and vice versa (Fig. 1(c)). Therefore, between two trajectories formed by turns of the same sign, another trajectory formed by turns of the opposite sign will always exist (Fig. 1(b) and (d)). This implies that two trajectories of the same sign can never cross.

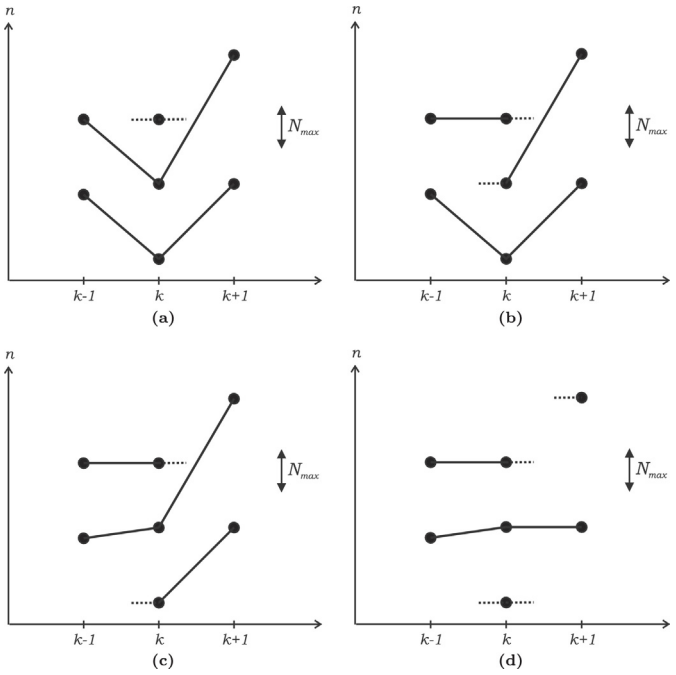

Fig. 4. Evolution of the trajectories in various stages of the algorithm for three consecutive spatial positions. Note that points represent real turns, solid lines represent unions between real turns, and dotted lines represent unions between real and phantom turns; (a) initialization of the trajectories according to the order of occurrence criterion; (b) first exchange in position k. The exchange that maximizes the STSR is selected; (c) second exchange in position k. After this exchange the STSR cannot increase with any other exchange and the algorithm jumps to the next position; (d) the exchange loop is executed in position $k+1$. Note that the union between two turns does not occur if the time shift is greater than N_{max}.

The merit figure used to evaluate trajectory point exchanges is the squared time-shift reduction (STSR), instead of the local smoothness deviation. The consecutive turns belonging to correctly-formed trajectories should have small time shifts, a situation which the STSR reflects better than local smoothness deviation does. The STSR caused by the exchange of the turns of position k between the trajectories i, j is defined as

$$r_k^{ij} = (s_k^{ii} + s_k^{jj}) - (s_k^{ij} + s_k^{ji}) \tag{4}$$

where

$$s_k^{ab} = |m_k^b - m_{k-1}^a|^2 \tag{5}$$

is the squared time shift between the turns p_{k-1}^a and p_k^b, with m_{k-1}^a and m_k^b being its respective instants of occurrence. During execution of the algorithm, exchanges that occur between pairs of trajectories that maximize the STSR (the reduction in squared time-shift) are accepted. The exchange process stops when no further exchange produces a positive STSR.

It is also necessary to define the STSR when any of the turns involved in the calculation are phantom turns. To this end, the algorithm assumes that the time shift between a phantom turn and any other turn is always N_{max}, the so-called maximum tracking interval threshold. This parameter imposes a maximum allowable time shift between a turn and the next turn within the same trajectory. In practice, a real turn will always be linked to a phantom turn if all the real turns in the next position are further away than N_{max}. In this way, the algorithm can generate incomplete trajectories comprising real and phantom turns (Fig. 4(b)–(d)).

The way in which STSR is defined ensures that the final trajectories do not cross. Exchanges that uncross crossed trajectories will always increase the STSR, and so, such exchanges will certainly be performed as the algorithm executes.

After running greedy exchange, our algorithm carries out an additional step to eliminate any trajectories with a number of turns smaller than a certain quantity L_{min}. The value of L_{min} is chosen such that any excluded short trajectories are more likely to be formed by false turn detections due to the presence of noise or artifacts than to be due to the presence of physiological activity.

2.3. Algorithm implementation

The steps of the MU profile extraction algorithm are:

2.3.1. Turn extraction

For each position k, n_k^q is the time of occurrence of the turn t_k^q. This turn is valid if and only if:

- t_k^q is a positive turn if some interval $n_a < n_k^q < n_b$ exists for which $V[k, n_k^q] = \max(V[k, n])$ in that interval and furthermore, $V[k, n_k^q] \geq V[k, n_a] + T_{thr}$, and $V[k, n_k^q] \geq V[k, n_b] + T_{thr}$.
- t_k^q is a negative turn if some interval $n_a < n_k^q < n_b$ exists for which $V[k, n_k^q] = \min(V[k, n])$ in that interval, and furthermore, $V[k, n_k^q] \leq V[k, n_a] - T_{thr}$, and $V[k, n_k^q] \leq V[k, n_b] - T_{thr}$.

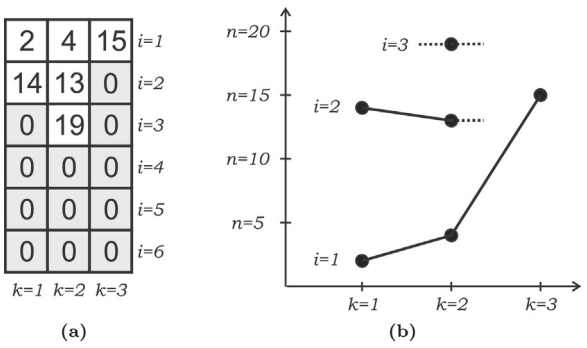

Fig. 5. Illustrative example of the initialization of the trajectories of the matrix M. In this example, two turns were detected in position $k=1$, at time 2 and 14; three turns were detected in $k=2$, at time 4, 13 and 19; and one turn was detected in $k=3$, at time 15; (a) representation of matrix M where, for each column, turn times are sorted in ascending order, and zeros are added to complete the column. Note that the size of the column is twice the maximum number of turns in a position (2×3 in this case). After the initialization, trajectories are arranged in rows. Note that trajectories may have both real (positives instants of occurrence in the matrix) and phantom turns (zeros in the matrix); (b) representation of all the trajectories with at least one real turn ($i=1$, $i=2$ and $i=3$), after the initialization. Points in the graph represent real turns, solid lines represent links between real turns, and dotted lines represent links between real and phantom turns.

where T_{thr} is the turn detection threshold. Note that for each position k, turns are ordered in time, satisfying $n_k^q < n_k^{q+1}$; $1 \le k \le K$.

2.3.2. Trajectory initialization

A matrix $M = \{m_k^i\}$; $1 \le k \le K$ containing the time of occurrence of the turns of a set of provisional trajectories is created. Each row of the matrix will contain one or several trajectories that will be modified during the execution of the algorithm. The matrix is initialized following the order of occurrence of the turns for each position (Figs. 4(a) and 5). Thus, in the kth column, the matrix will contain the time of occurrence of the turns of the kth position, in ascending order, followed by zeros to complete the column. Note that the zeros in the matrix represent phantom turns. The number of rows will be twice the number of turns at the recording position at which the highest number of turns is found. This ensures that every turn can be exchanged with a phantom turn during the execution of the algorithm. Mathematically:

$$m_k^i = \begin{cases} n_k^i & i \le Q_k \\ 0 & i > Q_k \end{cases} \tag{6}$$

where $1 \le k \le K$ and $1 \le i \le 2\max(Q_k)$.

2.3.3. Exchange loop

The matrix M is modified during this loop, according to the modified greedy exchange algorithm (Fig. 4(b)–(d)):

- $\forall k$; $2 \le k \le K$ (for each recording position)
  - While some exchange is possible:
    - $\forall i, j \in 1, \ldots, 2\max(Q_k)$; $i \ne j$ (for each combination of trajectory exchanges at position k):
      - Calculate the STSR of exchanging the elements m_k^i and m_k^j of the matrix M as:

$$r_k^{ij} = (s_k^{ii} + s_k^{jj}) - (s_k^{ij} + s_k^{ji})$$

$$s_k^{ab} = \begin{cases} |m_k^b - m_{k-1}^a|^2 & m_k^b, m_{k-1}^a \ne 0 \\ N_{\max}^2 & \text{otherwise} \end{cases} \tag{7}$$

where N_{max} is the maximum tracking interval threshold.

- Select among all possible exchanges, the exchange (i.e., the i_{max}, j_{max} pair) with maximum STSR.
- If the STSR for the selected exchange is positive, exchange the elements $m_k^{i\max}$ and $m_k^{j\max}$ of the matrix M. Otherwise, when no possible exchange with positive STSR exists, the loop jumps to the next recording position k.

2.3.4. Trajectories purging

The final step is to read the trajectories from the processed matrix. Each trajectory will be formed by sets of real turns in consecutive positions of a given row of the matrix. Note that, throughout the entire matrix, there may be more than one trajectory per row. For a trajectory to be considered valid, it must contain a minimum number of turns: all trajectories shorter than L_{min} are removed. Therefore, for a given i, the set $\{(k, m_k^i, V[k, m_k^i])\}$; $k_1^i \le k \le k_2^i$ is considered a valid trajectory, if it satisfies the following conditions:

- $m_k^i \ne 0 \forall k$; $k_1^i \le k \le k_2^i$
- $k_2^i - k_1^i + 1 \ge L_{\min}$
- $(m_{k_1^i - 1}^i = 0) \vee (k_1^i = 1)$
- $(m_{k_2^i + 1}^i = 0) \vee (k_2^i = K)$

where the first two conditions ensure a continuous trajectory of at least L_{min} turns, and the other two conditions ensure that the trajectory is delimited either by phantom turns or by the recording limits.

It is important to note that the steps described in Sections 2.3.2, 2.3.3, and 2.3.4 are performed separately for the set of positive and negative turns, in order to preclude the possibility of obtaining trajectories that contain both positive and negative turns.

Fig. 6 shows as an example the MU profile obtained by means the proposed algorithm from a real scanning-EMG signal. The parameter values used in this case were: T_{thr}=21.2 μV, N_{max}=9 samples and L_{min}=13 traces. The execution time of the algorithm (implemented in C running in Matlab R2015a) for this particular example was 10 ms which means that it is negligible compared to the typical scanning-EMG recording time, which is not less than one minute.

2.4. Algorithm evaluation

The performance of the proposed algorithm was studied by applying it to real scanning-EMG signals, and experimentation whilst carrying out these tests enabled an evaluation of how the algorithm's parameters affect its behavior.

2.4.1. Signal acquisition and processing

Twenty scanning-EMG signals were recorded from the biceps brachii of five normal subjects (3 male and 2 female) aged between 24 and 54 years. Informed consent was obtained from all subjects, and the study was approved by the ethics committee of Public University of Navarra. Scanning-EMG recordings were obtained following the recording protocol explained in detail elsewhere [4], with scanning steps of 50 μm and a sampling frequency of 20 kHz. A concentric needle was used as scanning electrode and a facial concentric needle was used as trigger electrode.

The raw signal was digitally processed to improve its quality [4]. Firstly, a band-pass filter in the time domain was applied. The lower cutoff frequency was between 10 Hz and 25 Hz, depending on the level of baseline noise of the scanning-EMG signal, and the upper cutoff frequency was 5 kHz for all signals. A median filter of 3, 5 or 7 points in the spatial domain was applied, depending on the artifact noise level of the scanning-EMG signal. The limits of the signal were

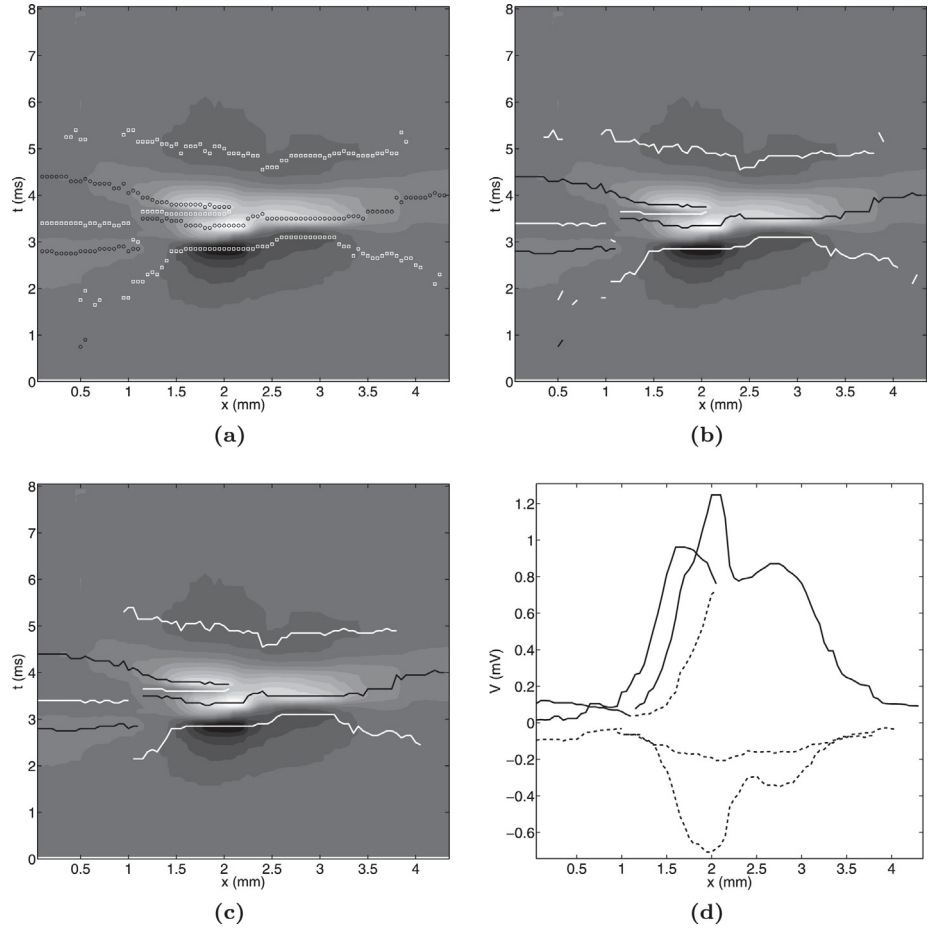

Fig. 6. (a) Representation of a recorded scanning-EMG signal in a contour plot in the time-space plane. Superimposed are depicted the positive turns (black circles) and negative turns (white squares) extracted from the signal; (b) the turns are linked to obtain a set of trajectories formed by positive turns (black lines) and a set of trajectories formed by negative turns (white lines); (c) trajectories shorter than L_{min} are eliminated. The depiction shows the definitive calculated MU profile in the time-space plane; (d) final MU profile depicted in the amplitude-space plane, with trajectories of positive turns represented by solid lines and trajectories of negative turns represented by dashed lines.

manually determined in both temporal and spatial dimensions so that it contained only the region of physiological activity.

2.4.2. MU profile gold standard definition

A gold standard MU profile for each scanning-EMG signal was manually obtained by an expert neurophysiologist with a view to establishing the criterion with which to quantify the quality of the MU profile obtained with the algorithm. Gold standard MU profiles were obtained using the following procedure:

- Turns of the scanning-EMG signal were automatically extracted following the definition provided in Section 2.3.1. The threshold T_{thr} was chosen manually, on the basis of the amplitude and the noise level of the scanning signal.
- Turns considered to be caused by noisy activity were removed by manual editing.
- Turns were added at spatio-temporal positions where it was considered that a local maxima or minima attributable to physiological activity was to be expected but had not been detected automatically. The expectation of maxima or minima due to physiological activity was based on observation of the waveforms of five spatially adjacent MUPs.
- Trajectories were obtained by manually linking the turns. In order to achieve smooth trajectories, turns located in zones in which the MUP waveform was relatively flat could be moved slightly on the time axis.

2.4.3. Merit figures

A link can be defined as a pair of consecutive turns of the same trajectory. Hence, the MU profile is the set of all the links of all its trajectories. The following merit figures were employed to quantify the quality of the MU profile provided by the algorithm:

- True positives (TPs): links included in the gold standard MU profile that were also included in the algorithmic MU profile.
- False positives (FPs): links not included in the gold standard MU profile but that were included in the algorithm MU profile.
- False negative (FNs): links included in the gold standard MU profile but that were not included in the algorithmic MU profile.
- Accuracy (A): calculated as [15]

$$A = \frac{TP}{TP + FP + FN} \tag{8}$$

An algorithmic link and a gold standard link were considered to correspond to each other if both turns forming the algorithmic link corresponded respectively to both turns forming the gold standard link, otherwise, the algorithmic MU profile was regarded to have a FP or a FN. An algorithmic turn and a gold standard turn were considered to correspond to each other if the following conditions were met:

- The spatial position of the two turns is the same.
- The difference between the instants of occurrence of the two turns is equal to or less than the duration of three samples,

Table 1
Ranges and values for the algorithm parameters.

Parameter	Variation range	Steps increment	Constant value
T_{thr} (μV)	8–148	5	27.8
N_{max} (samples)	0–18	1	5
L_{min} (traces)	1–20	1	7

which corresponds to ±0.15 ms. This allowance accommodates any small displacements made to smoothly link turns when manually obtaining the gold standard MU profile.
- The turn calculated by the algorithm does not correspond to any other turn of the gold standard MU profile, and vice versa.

2.4.4. Parameters influence

The first set of experiments studied how the calculation of the MU profile for a single scanning-EMG signal is affected by the values of the algorithm parameters. The three parameters of the algorithm are the turn detection threshold, T_{thr}; the maximum tracking interval threshold, N_{max}; and the trajectory purge threshold; L_{min}. Each parameter was varied while keeping the other two parameters constant (Table 1). For each parameter combination, the MU profile was obtained and the merit figures (*TP*, *FP*, *FN* and *A*) were calculated.

2.4.5. Optimal parameters values

A second set of experiments was performed with the aim of finding a set of default parameter values which can be routinely used by the algorithm. In order to achieve this, the parameter values that maximized the accuracy (we will henceforth refer to these values as optimal parameter values) were obtained for each of the 20 recorded scanning-EMG signals. A genetic algorithm was used for this purpose [16], using the following setting: the population size was 40; the number of individuals belonging to the elite was 2; the crossover probability was 0.8; and the number of generations was 300. The parameter search ranges were: $T_{thr} \in [0, 1000]$ μV; $N_{max} \in [0, 12]$ samples; $L_{min} \in [0, 30]$ traces. The accuracy achieved after the optimization process was the optimal accuracy.

Whilst the optimal parameter values obtained were the most appropriate parameters for a given scanning-EMG signal, they may not be optimal for other signals. With this in mind, the set of parameter values that maximized the averaged accuracy of all the selected scanning-EMG signals (global parameter values) was obtained, using the same optimization algorithm as that used with single signals. In order to study whether the global parameter values were suitable for use with a wide range of scanning-EMG signals, for each of the 20 recorded scanning-EMG signals, MU profiles were generated using the global parameter values and the accuracy of MU profile extraction (global accuracy) was calculated.

3. Results

3.1. Influence of the parameters

The results of the experiments described in Section 2.4.4 are shown in Fig. 7. With regard to the turn detection threshold, T_{thr}, if this was low, the FP value obtained was high and the FN value was

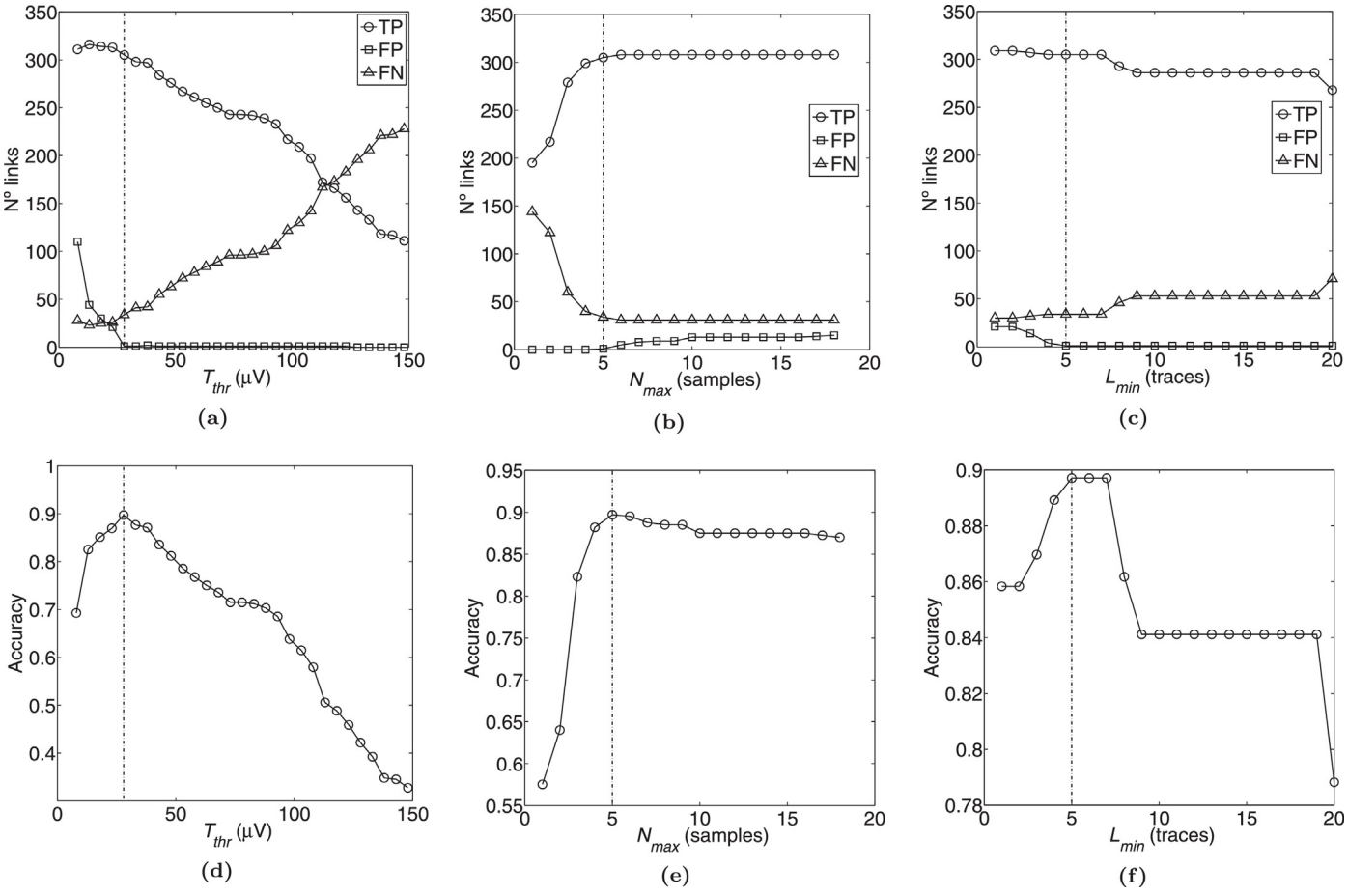

Fig. 7. Merit figures values obtained for a scanning-EMG signal: (a) TP (circles), FP (squares) and FN (triangles) obtained varying T_{thr} while N_{max} = 5 samples and L_{min} = 7 traces; (b) TP, FP and FN obtained varying N_{max} while T_{thr} = 27.8 μV and L_{min} = 7 traces; (c) TP, FP and FN obtained varying L_{min} while T_{thr} = 27.8 μV and N_{max} = 5 samples; (d) accuracy obtained varying T_{thr}; (e) accuracy obtained varying N_{max}. (f) accuracy obtained varying L_{min}. The dashed line in each figures indicates the parameter value that yielded maximum accuracy.

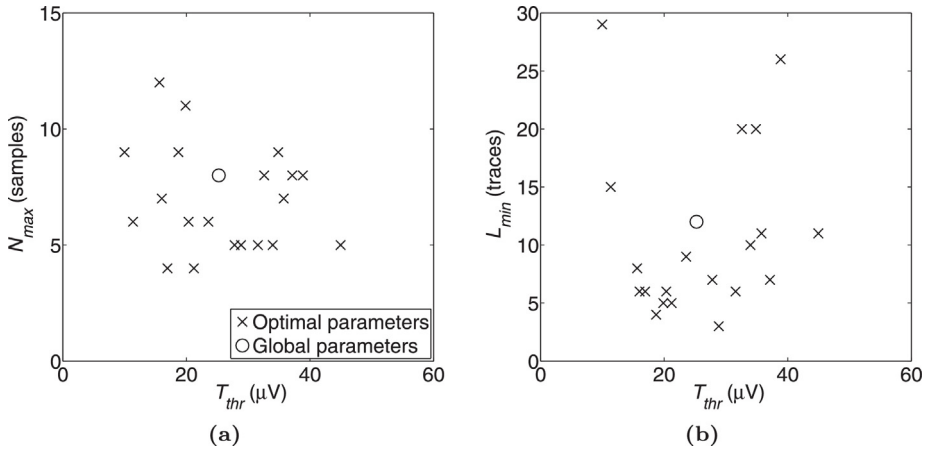

Fig. 8. Representation of the optimal parameters values (crosses) and the global parameters values (circles) obtained in the experiments in two projections of the parameter space.

low. As T_{thr} was increased, FN increased and from T_{thr} = 28 μV the FP decreased rapidly (Fig. 7(a)). This value of T_{thr}, where FP dropped, coincided with the maximum accuracy (Fig. 7(b)).

With regard to the maximum tracking interval threshold, N_{max}, if this was low, FP was 0 and FN was high. As N_{max} was increased, FP remained 0 and FN decreased until an N_{max} of 5 samples is reached. From this value FP increased slightly and FN was more or less constant (Fig 7(c)). This value of N_{max} = 5 coincided with the maximum accuracy (Fig. 7(d)).

Regarding the trajectory purge threshold, L_{min}, while this parameter was low, as it was increased, FP increased. However, if L_{min} was above about 5 traces, FP was approximately zero (Fig 7(e)). This value of L_{min} coincided with maximum accuracy (Fig. 7(f)). The value of FN increased as L_{min} was increased, and this occurred over the whole L_{min} range (Fig 7(e)).

Accuracy was affected in a similar way by all of the three parameters. At the lower ends of the ranges of the parameters, accuracy rapidly increased as the parameter values were increased, until a maximum accuracy was reached (at T_{thr} = 28 μV, N_{max} = 5 samples, L_{min} = 5 traces). Further increases of parameter values resulted in progressively lower accuracy figures (Fig. 7(b), (d) and (f)).

3.2. Optimal parameters values

Fig. 8 presents the results of experiments to find the optimal parameter values for each of the 20 recorded scanning-EMG signals (Section 2.4.5). Note that, although the optimal parameter values were widely spread in the parameter space, the global parameter values (T_{thr} = 25.2 μV, N_{max} = 8 samples, L_{min} = 12 traces) were located approximately in the center of the range of variation of the optimal parameter values.

Fig. 9 shows global accuracy and optimal accuracy for the different scanning-EMG signals. Optimal accuracy ranged between 0.78 and 0.98 (Fig. 9(c)), and global accuracy ranged between 0.7 and 0.93 (Fig. 9(d)). The accuracy loss was small for most of scanning-EMG signals, being below 0.1 for 75% of the signals and below 0.05 for 33% of the signals (Fig. 9(b)).

4. Discussion

4.1. MU profile usefulness

The MU profile is a new concept for characterization of complexity of the MU by identifying the trajectories of positive and negative turns of the scanning-EMG signal in the temporal dimension. Thus, the MU profile can be understood as a bi-dimensional extension of the concept of turn. Through identification of trajectories, useful information about MU structure is obtained from both from the space-time projection (Fig. 6(c)) and the space-amplitude projection (Fig. 6(d)).

The space-time projection gives information about the relative delay between the trajectories forming the MU profile. Previously-defined scanning-EMG parameters, such as, temporal delay between MU fractions [7] can easily be calculated from this projection. Temporal delay between fractions provides information about synchronization of the single fiber action potentials of MU fibers; the temporal delay depends on the distance from the neuromuscular junction to the recording site, muscle fiber conduction velocity and characteristics of the initiation of depolarization. As conduction velocity should not systematically change between fractions of the same MU, and as delays in the initiation of depolarization are negligible in comparison to propagation delay, the most probable cause for systematic non-synchronization between MU fractions is that different fibers are in different innervation zones with different axonal branches, each of which has a different delay [5].

The space-amplitude projection gives information about the amplitude decline as a function of the recording position within the corridor, i.e., amplitude change with recording distance [13,14]. In this projection, each amplitude maximum is associated with a certain spatial position and indicates the depth of the set of fibers that is contributing to the trajectory of the MU profile. Three variables can affect the maximum amplitude and the steepness of the decay of the trajectory: the number of muscle fibers contributing coherently, their distance from the scanning corridor and their diameters. In general, a high maximum amplitude corresponds to a large number of fibers, to several fibers that are close together or to fibers of large diameter. A steep decay corresponds to fibers being close together.

The MU profile can also provide information about other scanning-EMG parameters, such as, the number and length of MU fractions, the number and length of silent zones, the number and length of polyphasic fractions or the length of the MU territory [7,6]. For instance, MU fractions can be related with groups of trajectories in a certain spatial region. If the number of coexisting trajectories is high, it can be inferred that the fractions are polyphasic. Silent areas can be related with spatial regions without trajectories or with very low amplitude trajectories, which are located between regions with much higher amplitude trajectories.

The MU profile is expected to reflect changes in the anatomy and physiology of the MU in pathological processes. For example, in neuropathy, because of reinnervation of muscle fibers, MUs generally have a higher fiber density [17], and therefore the MU profile is

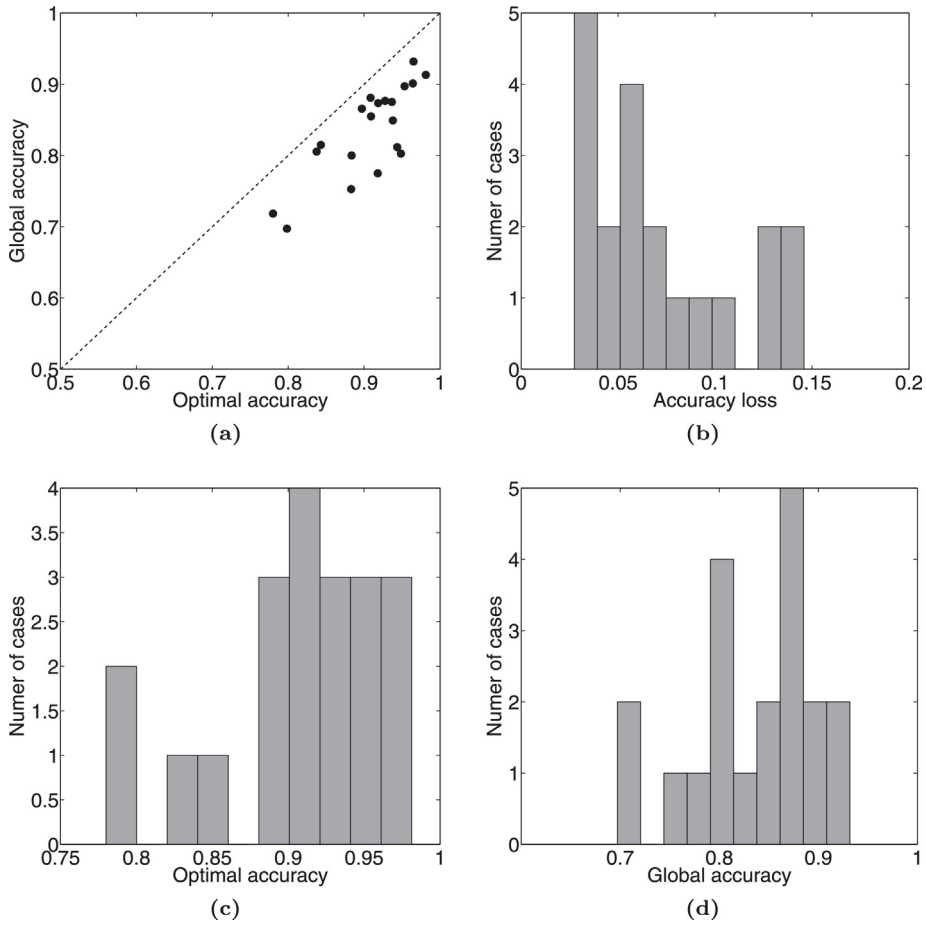

Fig. 9. Optimal accuracy and global accuracy obtained for each scanning-EMG signal: (a) representation in the plane of optimal accuracy vs. global accuracy. Note that axis range is from 0.5 to 1. Each point represents the results of a specific scanning-EMG signal. The dashed line represents the ideal case in which there would be no loss of accuracy; (b) histogram of the values of accuracy loss (optimal accuracy – global accuracy); (c) histogram of the values of optimal accuracy; (d) histogram of the values of global accuracy.

expected to have higher maximum amplitudes than those observed in the MU profile of a healthy individual. Reinnervation also results in more complex MUs, implying an increase in waveform complexity [18,19] and an increase in the number of polyphasic fractions [6] with respect to normal conditions. Consequently, the MU profile is expected to contain recording regions in which there is coexistence of large numbers of trajectories.

Under myopathy, processes such as fiber loss, fiber atrophy and hypertrophy, and fiber splitting occur [20]. Loss of muscle fibers tends to reduce the amplitude of the scanning-EMG signal [20,18] and therefore the same should occur with the MU profile amplitude. Loss of muscle fibers results in an increase in the number and size of silent areas [6,11], and these changes will be reflected in the MU profile.

In short, the MU profile provides a concise, numerical summary of information about the complexity of the scanning-EMG signal. Because complexity is closely related to the anatomy and physiology of the MU, the MU profile is a promising tool for the analysis of pathological change in the MU.

4.2. Algorithm sensitivity to parameter values

The MU profile algorithm has three parameters that must be set before being run. The values of these parameters significantly affects how accurately the algorithm extracts MU profiles. If the turn detection threshold T_{thr} is low in relation to the noise level, then some of the noise may be interpreted as being signal turns [1]. If the same false turns are detected in several consecutive positions, the result can be inaccurate trajectories and a MU profile with a number of FPs (Fig. 7(a)). Choosing a higher T_{thr} can help to decrease the number of false turns, but if T_{thr} is too high, the detail in the scanning-EMG signal will be lost because some of the real turns will not be detected, and there will be a number of FNs (Fig. 7(a)).

Although spatial correlation of noise is induced to some degree by the median filtering used to preprocess the scanning-EMG signal, it can be assumed that noise in the signal is random and almost uncorrelated in the spatial dimension. Thus, the timing of noise bursts detected as false turns should be random and uncorrelated, and the temporal distance between false turns will also be random. If the maximum tracking interval threshold N_{max} is small enough, most false turns will be prevented from forming part of the same trajectory, and consequently, in general, the trajectories due to noise will be constituted by a small number of (false) turns. Such trajectories can be removed by choosing an appropriate value for the trajectory purge threshold, L_{min}; for the scanning-EMG signal in Fig. 7(e), for example, FP was negligible for values of L_{min} greater than 4 traces.

The degree of fragmentation of the trajectories in the MU profile is closely related to the value of N_{max}. If N_{max} is too low, turns associated with physiological activity are not tracked completely through the different corridor positions. The resulting trajectories will be short, and even if L_{min} is small they may be discarded; the extracted MU profile will thus have FNs (Fig. 7(c)). If, on the other hand, N_{max} is high, there is an increased possibility of false turns being accepted into trajectories, and, for this reason, the number of FPs increases with increasing N_{max} (Fig. 7(c)).

4.3. Optimal parameters values

The optimal values of the parameters will depend on the recording conditions used for the scanning signal. Important aspects include the sampling frequency, the distance between consecutive recording positions and the noise level of the recorded signal. In the experiments reported here, sampling frequency and spatial steps were always the same, but the nature and level of noise in the 20 signals were not. These differences explain why the optimal parameter values were found to differ for different recordings (Fig. 8) and highlight the desirability of having a set of parameter values acceptable for as wide a range of recording conditions as possible. Note that from the point of view of the user, it is important to find a set of default parameter values that can be routinely used. The global parameter values obtained for our set of signals (T_{thr} = 25.2 μV, N_{max} = 8 samples and L_{min} = 12 traces) were located in approximately the center of the respective ranges of the optimal parameter values. While there were evident differences among the optimal parameter values and the global ones, the accuracy obtained with the global parameter values was in all cases still acceptable (Fig. 9(d)) and the accuracy loss was small (Fig. 9(b)). In summary, the global parameter values were acceptable for the scanning-EMG signals used in the study, but MU profile quality could be improved by tweaking the values for each particular recording. Global parameter values can serve as an acceptable default setup or as a useful starting point from which to manually or automatically refine the algorithm.

5. Conclusion

The MU profile provides a way to visualize and quantify relevant information in a scanning-EMG signal. A formal definition of this new concept has been given, and an algorithm for extraction of the MU profile from standard scanning-EMG recordings has been developed and described. Preliminarily tests involving application of the algorithm to 20 real recordings provide promising proof of concept and established a set of default values for the algorithm's three parameters.

Acknowledgement

This work has been supported by the Spanish Ministerio de Economía y Competitividad (MINECO), under the TEC2014-58947-R project.

References

[1] E. Stålberg, S. Andreassen, B. Falck, H. Lang, A. Rosenfalck, W. Trojaborg, Quantitative analysis of individual motor unit potentials: a proposition for standardized terminology and criteria for measurement, J. Clin. Neurophysiol. 3 (4) (1986) 313–348.
[2] E. Stålberg, S.D. Nandedkar, D.B. Sanders, B. Falck, Quantitative motor unit potential analysis, J. Clin. Neurophysiol. 13 (5) (1996) 401–422.
[3] E. Zalewska, I. Hausmanowa-Petrusewicz, Evaluation of muap shape irregularity–a new concept of quantification, IEEE Trans. Biomed. Eng. 42 (6) (1995) 616–620.
[4] E. Stålberg, L. Antoni, Electrophysiological cross section of the motor unit, J. Neurol. Neurosurg. Psychiatry 43 (6) (1980) 469–474.
[5] J. Navallas, E. Stålberg, Studying motor end-plate topography by means of scanning-electromyography, Clin. Neurophysiol. 120 (7) (2009) 1335–1341.
[6] E. Stålberg, P. Dioszeghy, Scanning EMG in normal muscle and in neuromuscular disorders, Electroencephalogr. Clin. Neurophysiol./Evoked Potentials Sect. 81 (6) (1991) 403–416.
[7] T. Gootzen, Electrophy siological investigation of motor unit structure by means of scanning EMG, in: Muscle Fibre and Motor Unit Action Potentials. A Biophysical Basis for Clincal Electromyography, 1990, pp. 89–106.
[8] I.K. Sethi, R. Jain, Finding trajectories of feature points in a monocular image sequence, IEEE Trans. Pattern Anal. Mach. Intell. (1) (1987) 56–73.
[9] V. Salari, I.K. Sethi, Feature point correspondence in the presence of occlusion, IEEE Trans. Pattern Anal. Mach. Intell. (1) (1990) 87–91.
[10] J. Navallas, J. Rodríguez, E. Stålberg, EMG Methods for Evaluating Muscle and Nerve Function, INTECH Open Access Publisher, 2012, Ch. 24.
[11] P. Dioszeghy, Scanning electromyography, Muscle Nerve 25 (S11) (2002) S66–S71.
[12] A. Yilmaz, O. Javed, M. Shah, Object tracking: a survey, ACM Comput. Surv. (CSUR) 38 (4) (2006) 13.
[13] D. Dumitru, J.C. King, S.D. Nandedkar, Concentric/monopolar needle electrode modeling: spatial recording territory and physiologic implications, Electroencephalogr. Clin. Neurophysiol./Electromyogr. Motor Control 105 (5) (1997) 370–378.
[14] S.D. Nandedkar, Models and simulations in electromyography, Muscle Nerve 25 (S11) (2002) S46–S54.
[15] C.E. Metz, Basic principles of roc analysis, in: Seminars in Nuclear Medicine, Elsevier, 1978, pp. 283–298.
[16] D.E. Goldberg, Genetic Algorithms in Search, Optimization and Machine Learning, 1989, Reading, MA.
[17] E. Kugelberg, L. Edström, M. Abbruzzese, Mapping of motor units in experimentally reinnervated rat muscle interpretation of histochemical and atrophic fibre patterns in neurogenic lesions, J. Neurol. Neurosurg. Psychiatry 33 (3) (1970) 319–329.
[18] E. Stålberg, B. Falck, The role of electromyography in neurology, Electroencephalogr. Clin. Neurophysiol. 103 (6) (1997) 579–598.
[19] E. Zalewska, I. Hausmanowa-Petrusewicz, Effectiveness of motor unit potentials classification using various parameters and indexes, Clin. Neurophysiol. 111 (8) (2000) 1380–1387.
[20] P. Hilton-Brown, E. Stålberg, The motor unit in muscular dystrophy, a single fibre EMG and scanning EMG study, J. Neurol. Neurosurg. Psychiatry 46 (11) (1983) 981–995.